Global Potential Energy Contour Plots for Chemical Reactions. Stepwise vs Concerted 2 + 2 Cycloaddition

R. A. Marcus

Contribution No. 9002 from Noyes Laboratory of Chemical Physics, California Institute of Technology, Pasadena, California 91125

Received October 21, 1994[®]

Abstract: A global contour plot is described for reactions involving stepwise or concerted addition of two ethylenes to form cyclobutane. The relevant isomers of the various species and of the reaction paths, with plains or valleys, minima, saddle points, and domes or conical intersections, are described. Two collective asymmetric coordinates are introduced as axes for the plot, which presents an overview of the system and which complements the usual 2-dimensional cuts of the many-dimensional potential energy surface. Other global coordinates are also introduced. The plot involves a pointwise minimization of the potential energy with respect to the coordinates not used as axes. A permutation symmetry can be used to derive the various coordinates. Free energy and entropy (or number of states) curves versus a reaction coordinate are discussed.

Introduction

In a previous paper a global potential energy contour plot was described, using several chemical reactions as examples. Systems with a number of isomers of the reactants, products, intermediates, and transition states were depicted using such a plot. It focuses on the overall topography of the potential energy surface and provides a "bird's eye view" of the various alternative paths in the reacting system. It complements, thereby, the typical 2-coordinate cuts of the potential energy surfaces that are functions of the many internal coordinates, 3n - 6 for an n atom nonlinear system.

In the present article these arguments are extended to the 2 + 2 cycloaddition, the combination of two ethylene-like molecules to form a cyclobutane-like molecule, either in a concerted or in a stepwise manner, the latter involving a diradical intermediate. The reactions are represented schematically by eqs 1 and 2:

where the diradical in eq 2 may be gauche or trans and where actual changes in bond lengths and angles are not indicated.

Aspects such as Woodward-Hoffmann orbital symmetry considerations have been examined in the literature of potential energy surfaces and play a role in such systems. Recently Zewail and co-workers² observed and measured in real time the conversion of the diradical, prepared in a different manner, to two ethylenes or to cyclobutane. The present work was prompted by such experiments and by electronic structure calculations and detailed analyses of potential energy surfaces by Bernardi, Robb, and co-workers for the 2+2 cycloaddition

system.^{3,4} We also draw upon the detailed calculations of Doubleday.⁵

Global Potential Energy Contours

Introduction. The system considered involves a pair of ethylene-like molecules, four diradicals, and one cyclobutane-like molecule (Figure 2, given later). Using a single "global" potential energy contour diagram, we wish to depict all such structures, their transformations into each other, the different reaction paths involved, and the overall topography of the surface. We also wish to consider reaction coordinate plots of the free energy (canonical system) or entropy (microcanonical), their construction, and their use in transition state theory for a canonical system and in RRKM theory for a microcanonical one.

In a global potential energy contour plot, topographical features such as valleys or plains, minima, domes or cones (conical intersections), and saddle points may be depicted for the entire system, including those of the relevant isomers. When the system is not exactly symmetric, similar considerations may remain applicable: In principle at least, properties, such as minima, saddle points, domes, and conical intersections of a less symmetrical system can be mapped onto those of the corresponding symmetric one and used as a guide for choosing suitable coordinate axes for the plot for the less symmetrical system.

In current quantum electronic structure studies, the potential energy surface has been calculated for a possible concerted reaction of two ethylenes, reaction 1, and for a stepwise mechanism involving instead a diradical intermediate, reaction 2 (e.g., refs 3-5). For the four carbons there are 3n-6, or six, relevant internal coordinates, plus 24 additional internal coordinates of the four methylenes. A first task in making the global plot is to select from these thirty coordinates two that are particularly suitable for its construction. Usually, they will be collective asymmetric coordinates. The coordinates differ

[⊗] Abstract published in Advance ACS Abstracts, April 15, 1995.

⁽¹⁾ Marcus, R. A. J. Phys. Chem. 1991, 95, 8236.

⁽²⁾ Pedersen, S.; Herek, J. L.; Zewail, A. H. Science 1994, 266, 1359.

⁽³⁾ Bernardi, F.; De, S.; Olivucci, M.; Robb, M. A. J. Am. Chem. Soc. 1990, 112, 1737.

⁽⁴⁾ Bernardi, F.; Bottoni, A.; Robb, M. A.; Schlegel, H. B.; Tonachini, G. J. Am. Chem. Soc. 1985, 107, 2260.

⁽⁵⁾ Doubleday, C. J. Am. Chem. Soc. 1993, 115, 11968.

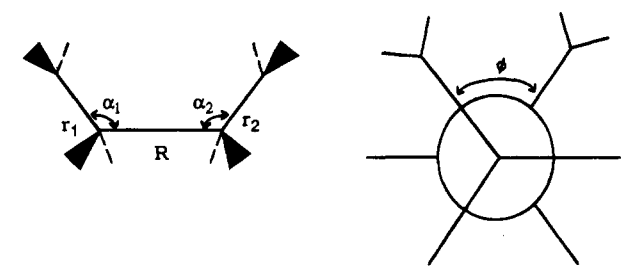


Figure 1. Typical coordinates for a pair of ethylenes.⁴ The wedges and the dashes denote CH bonds, and the angles and lengths are not drawn to scale.

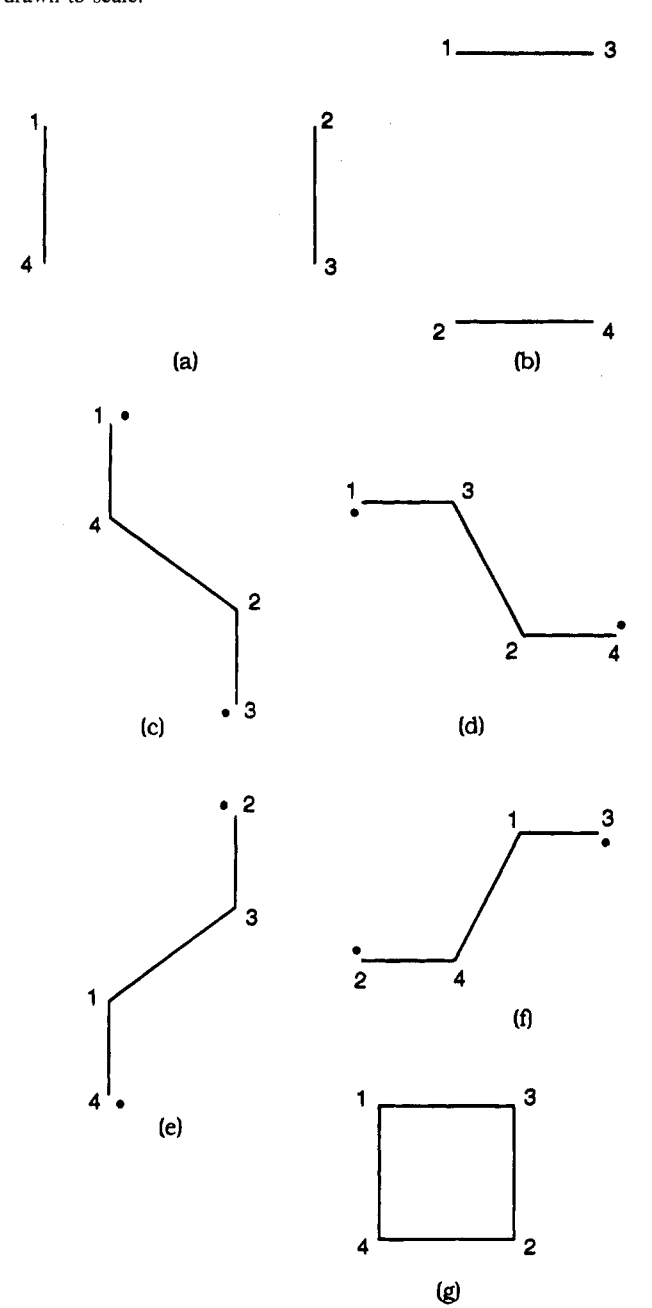


Figure 2. Structure for a and b ethylene pairs (each line representing a double bond, in this case only); c-f diradicals, and (g) cyclobutane.

from the internal coordinates typically used for the four carbons in reactions 1 and 2: r_1 , r_2 , α_1 , α_2 , R, and ϕ , given in Figure 1 and taken from ref 4 (Scheme III there). The geometries considered in ref 4 mainly have $r_2 = r_1$ and $\alpha_2 = \alpha_1$, as in the configurations in Figure 2. We first give the global coordinates for a trans attachment of the ethylenes and in a later section those for a gauche attachment.

Coordinates and Regions in the Global Plot. A trans attachment of the pair of ethylenes in Figure 2a yields the diradicals in Figures 2b and 2c. A subsequent transition to the gauche form to permit a cyclization yields the cyclobutane in Figure 2g. (In any structure in Figure 2 only the internuclear distances are specified, the spatial orientation of the structure as a whole being arbitrary.) From this cyclobutane the diradicals in Figures 2d and 2f can be generated and from them the ethylene pair in Figure 2b.

A global plot will include all the structures in Figure 2. Coordinates can be selected so that the cyclobutane occupies the center, the four diradicals each of the four quadrants, and the two ethylene pairs the regions at either end of a coordinate axis. Initially, I obtained the six coordinates given below intuitively, but subsequently showed that they could be obtained, instead, systematically, using a particular permutation symmetry. The latter derivation is given later in this section.

The coordinates q_1 and q_2 chosen as axes for the plot are

$$q_1 = \frac{1}{2}[(r_{14} + r_{23}) - (r_{13} + r_{24})] \tag{3}$$

$$q_2 = \frac{1}{2}[(r_{14} + r_{13}) - (r_{23} + r_{24})] \tag{4}$$

The normalization factors and those in q_3 to q_6 given below make the transformation, which is an orthogonal one, distance conserving (cf. Appendix A).

One role of q_1 is to serve as a separation distance coordinate for each pair of ethylenes in Figure 3. Another, it will be seen, is to serve as a major component of the reaction coordinate in the saddle-point region for the formation of the trans diradical. Each r_{ij} denotes the distance between the atoms (i, j). In the global plot the 4 remaining carbon coordinates and the 24 internal ones of the CH₂'s are adjusted pointwise so as to minimize the potential energy at each value of (q_1, q_2) . Functions of r_{ij} such as r_{ij}^2 could be used in eqs 3 and 4 instead of r_{ij} . In the minimization, resulting in a projection of a 30-dimensional plot onto 2, a nearby local minimum rather than an absolute one is selected, such as to maintain a physical continuity of each reaction path.

It is supposed in Figure 3 that to yield a better reaction path there is no advantage in having a 90° rotation of one ethylene relative to the other *prior* to the formation of a diradical. In this way, from each configuration of the ethylenes in Figure 3 only two paths for diradical formation need be considered in constructing the plot, instead of four. One problem which exists when a many-dimensional plot is projected onto a two-dimensional one is that various originally separate paths and structures may now overlap on the projected space. This problem is avoided by this condition in Figure 3.

Keating and Mead⁶ noted that for n=3 and 4, the number of independent distances n(n-1)/2 equals the number of internal coordinates of a nonlinear system, 3n-6, so these distances or functions of them could be used for the coordinates in these two cases. For their particular purpose they used r_{ij}^{2} 's instead of r_{ij} 's in their choice of six coordinates, which partly differed from ours since they were interested in the properties of the full S_4 permutation group.⁶ Those coordinates do not have the symmetry properties desirable for the present global plot, which involves particular permutations and a different goal.

For the four remaining coordinates for the four carbons we introduce q_3 to q_6 :

$$q_3 = {}^{1}/_{2}[(r_{14} + r_{24}) - (r_{13} + r_{23})]$$
 (5)

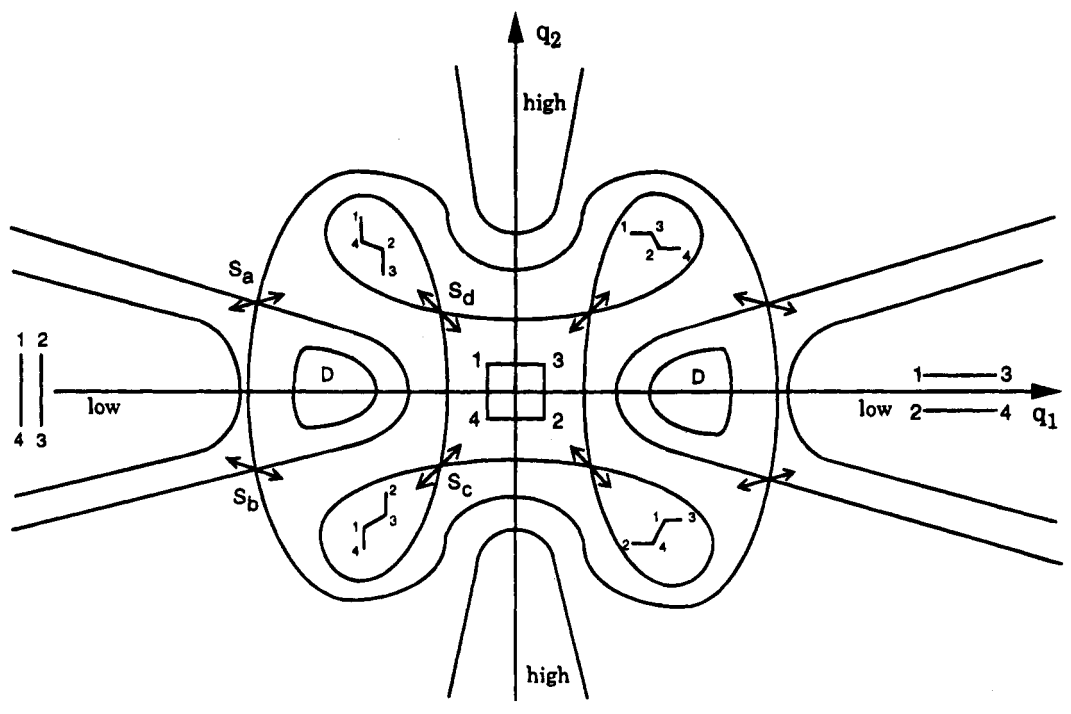


Figure 3. Global contour plot for reactions 1 and 2 when the attachment of the ethylene pairs is trans.

$$q_4 = \frac{1}{2}[r_{13} + r_{14} + r_{23} + r_{24}] \tag{6}$$

$$q_5 = \frac{1}{\sqrt{2}}(r_{12} - r_{34}) \tag{7}$$

$$q_6 = \frac{1}{\sqrt{2}}(r_{12} + r_{34}) \tag{8}$$

where q_3 is another asymmetric coordinate, q_4 is a symmetric "breathing" coordinate, and q_5 is asymmetric and q_6 symmetric in r_{12} and r_{34} , the two coordinates not present in q_1 to q_4 . The inverse of the transformation, namely from the q's to the r's, is given in Appendix A.

Of these coordinates q_5 is zero for all of the structures specifically depicted in Figures 2 and 3. The asymmetric stretching coordinate q_3 is seen from eq 5 and Figure 2 to vanish, like q_2 , for the face-to-face geometry of the two pairs of ethylenes and for the cyclobutane (puckered or not). Had the diradical structure in Figure 2f been placed in the upper right instead of the lower right quadrant of Figure 3, q_3 rather than q_2 would have been the appropriate axis for that figure. The coordinate q_6 has the same value for all four diradicals. Its value for one ethylene pair is also the same as for the other. A similar remark applies to q_4 . The puckering angle in C_4H_{10} can be expressed in terms of the ratio q_4/q_6 : $q_4^2 = q_6^2$ for a planar C_4H_{10} and $q_4^2 > q_6^2$ for a puckered one.

In the two broad plains in Figure 3 the minimization of the potential energy V at any given q_1 and q_2 fixes the values of only r_{14} and r_{23} . It thus leaves as arbitrary there the values of two of six coordinates, for the given q_1 and q_2 .

The coordinates q_1 and q_2 are antisymmetric and q_3 to q_6 are symmetric with respect to the interchange of atoms 1 and 2, i.e., with respect to the permutation (12); q_1 and q_3 are antisymmetric and the other q's are symmetric with respect to the permutation (34). These results can be used to generate from any one structure in Figure 2 all equivalent structures there and to generate from one quadrant in Figure 3 the remaining three quadrants, remembering that only the internuclear distances in the global plot are specified, the spatial orientation of any structure being arbitrary. For any given numbering in a

cyclobutane there are two buckled isomers, mirror images of each other and each thermally accessible from the other. (The barrier is about 510 cm⁻¹.)⁷

This permutation symmetry in Figure 2 can be used to define q_1 to q_4 uniquely, apart from normalization: To generate q_1 to q_4 from the permutations (12) and (34) only the four r_{ij} 's which are altered by these permutations are considered, that is, r_{12} and r_{34} are excluded. There are only four combinations of r_{ij} 's which show symmetry or antisymmetry with respect to these two permutations. They are the q_1 to q_4 defined in eqs 3–6. The remaining two coordinates q_5 and q_6 provide the simplest complement to q_1 to q_4 which preserves orthogonality.

For comparison with a simpler system O_3 (e.g., ref 1 and references cited therein), where there are only three coordinates, we note that the basic configuration there is an equilateral triangle. (The coordinates q_1 to q_6 can be regarded as deformations of a square.) The two coordinates used to distort the triangle in the global plot are two asymmetric stretches, while the third coordinate, a symmetric stretch, can be adjusted pointwise so as to minimize the potential energy or can be held fixed. The global plot has three symmetrically related configurations of ozone, each an isosceles triangle with three saddle points separating them and one conical intersection at the center of the triangle.

The plot in Figure 3 describes reactions 1 and 2, with reaction 2 considerably favored, and contains the isomeric structures present in Figure 2, together with the reaction paths involving them. In Figure 3 two broad plains are seen which correspond to the two pairs of C_2H_4 's. They have the face-to-face structure depicted in Figures 2a and 2b, when $q_2 = q_3 = q_5 = 0$. There are also four regions corresponding to the four diradicals, with the structures indicated in Figures 2c-2f, and a central potential energy minimum, corresponding to the C_4H_8 in Figure 2g. The assignment of these particular structures to the various regions in Figure 3 can be made with the aid of eqs 3 and 4 as follows, letting q_3-q_6 vary as needed:

When the systems is in the form of the (14, 23) pair of C_2H_4 's, drawn in Figures 2 and 3, r_{13} and r_{24} in Figure 2a are relatively large compared with r_{14} and r_{23} , while $r_{13} = r_{24}$ and $r_{14} = r_{23}$

⁽⁷⁾ Egawa, T.; Fukuyama, T.; Yamamoto, S.; Takabayashi, F.; Kambara, H.; Ueda, T.; Kuchitsu, K. J. Chem. Phys. 1987, 86, 6018.

in a face-to-face geometry. It follows from eqs 3 and 4 that q_1 is fairly large and negative, and that $q_2=0$ for the face-to-face geometry. (For nonequal values of r_{13} and r_{14} at large $|q_1|$, however, q_2 is typically not zero, and so we have a broad plain.) This pair of ethylenes occupies the left-hand plain in Figure 3. The pair of ethylenes depicted in Figure 2b occupies the right-hand plain, as can be seen by arguing directly as above or using a permutation argument. (For example, a permutation (12) leads to a change of sign of q_1 , and leaves $q_2=0$ intact, with the other q's changing as needed. It leads to the given labels in the ethylene pair in the right side of Figure 3, remembering that one can rotate the pair as a whole.)

When the diradical intermediate has the structure given schematically in the upper left quadrant of Figure 3 (cf. Figure 2c), $r_{13} + r_{24}$ exceeds $r_{14} + r_{23}$, and so q_1 is negative. Since r_{13} is also larger than r_{24} in that Figure, while $r_{14} = r_{23}$, q_2 is moderately large and positive. The depicted diradical structure therefore occupies the upper left region in Figure 3. The other three diradicals in Figures 2d to 2f are assigned to the regions indicated in Figure 3, again either arguing directly or using a permutation argument.

Considering next the region in Figure 3 occupied by the cyclobutane, the appropriate sequence of the numbers of the atoms (apart from any overall rotation of the structure) is as given in Figures 2g and 3: Only this structure has $r_{13} = r_{23} = r_{14} = r_{24}$ and hence, according to eqs 3 and 4, only it can exist at the origin, $q_1 = q_2 = 0$. Any permutation of the numbering, apart from that equivalent to an overall rotation, would correspond to a different point in (q_1, q_2) space.

Reaction Paths, Saddle Points, Separatrices, and Domes. In Figure 3, each broad plain occupied by a pair of ethylenes is separated from a nearby diradical region by a saddle-point region, and with it a separatrix. The reaction path for the first step of reaction 2 proceeds from the left-hand plain to the upper left or lower left diradical region, as indicated by the arrow (really a phalanx of arrows) crossing the saddle-point region. The second step in reaction 2 is the passage from that diradical region to the central C_4 minimum in the figure. In ref 3, there is a small local maximum en route, resulting in a saddle-point region and hence in a separatrix, as in Figure 3. It will be noted that at each saddle point the contour lines cross (e.g., Appendix B) and form, thereby, the arms of a separatrix. There are also seen in Figure 3 three other symmetrically related saddle points and reaction paths from a pair of ethylenes to a diradical. However, whether a saddle point survives an energy minimization is discussed in Appendix B and considered later in this article.

We describe next the reaction paths in Figure 3, the first being between the left-hand ethylene pair and the trans diradical in the upper left region of the figure. In proceeding from that ethylene pair to this diradical, r_{13} and r_{24} decrease, r_{24} more than r_{13} , and then r_{14} and r_{23} increase slightly. The system reaches the saddle-point S_a in the upper left region. These r_{ij} changes are seen from eqs 3 and 4 to lead mainly to the q_1 becoming less negative and q_2 becoming somewhat positive. The reaction path in the vicinity of the saddle-point S_a thus has both a q_1 and q_2 component, as indicated schematically in Figure 3. Either arguing directly as above or using a permutation argument, the reaction paths indicated in the vicinity of the three corresponding saddle points in Figure 3 are obtained.

According to the calculations in refs 4 and 5, the trans form of the diradicals depicted in Figures 2c-2f has a slightly lower potential energy than the gauche form. Along the reaction path leading to the cyclobutane from any of the diradicals the diradical will, with the pointwise minimization of the potential energy along the path, change from trans to gauche and so

permit ring closure to occur. We consider later the saddle point between the trans and gauche conformations of the diradical.

The saddle-point S_d separates the gauche diradical from the cyclobutane region in the upper left quadrant. The r_{13} is the coordinate principally changing there on passage across S_d and is seen from eqs 3 and 4 to have both a q_1 and a q_2 component, as indicated by the arrow at that S_d saddle-point region. Related remarks apply to the corresponding three gauche diradical-cyclobutane saddle points in the other quadrants.

There are two "domes" D drawn in Figure 3, which block the direct path from each ethylene-pair plain to the central minimum. Each dome is an island created by being enclosed by the contours joining the saddle points surrounding it (the S's in the case of the dome on the left side of Figure 3). It can be seen from the numbering of the atoms in each ethylene pair and in the cyclobutane that a very large internal rotation of the ethylene pairs of about 180° (perhaps less by twice the dihedral puckering angle⁷ of 28°) would have to occur in order to reach the point $q_1 = q_2 = 0$ from large $|q_1|$ along the q_1 axis. However, the calculations in ref 4 indicate that the $[2_s + 2_a]$ formation of cyclobutane involves only a relatively small angle of internal rotation ($\sim 40^{\circ}$) to reach the saddle point and so corresponds, instead, to a saddle point given later in Figure 4. Thus, in Figure 3 there is a very large barrier, indicated by a high dome D, which may have a more complicated structure and which is presumably higher than the barrier at the saddle point on the x axis in Figure 4. As in Figure 4, the diagram is, in the absence of calculations of the minimized surface, partly a guess from the available calculations.

The trans-gauche diradical transition and its saddle point in each of the four quadrants of Figure 3 (not shown) are explored next: Certain of the q_i coordinates can be shown to have a "global φ " component, i.e., to have a component from internal rotation about the central CC bond in the diradical: The trans diradical structures in Figures 2c-2f may be compared with the corresponding gauche structures by rotating by 180° in Figures 2c-2e the line joining atoms 2 and 3 about the 2-4 axis, and by rotating by 180° in Figures 2d-2f the line joining atoms 2 and 4 about the 1-4 axis. The principal change in the upper left diradical is in r_{13} . We see from eqs 3-6 that q_1-q_4 all contain the reaction coordinate for the 180° rotation (r_{13} in the upper left quadrant, r_{14} in the upper right, etc.). Therefore, q_1 to q_4 all contain a "global φ " component. The separatrix will appear in each case in a minimized plot only if the local reaction coordinate is not a major component of the minimized variables, the amount permissible depending on ratios of the various local force constants (Appendix B).

The two-dimensional global plot in Figure 3 can be extended to a three-dimensional transparent model, using as coordinate axes the three asymmetric coordinates q_1-q_3 . It would have contour surfaces (equipotential surfaces) instead of contour lines, and the pointwise minimization would now be with respect to q_4-q_6 . The four radicals would occupy four of the octants of the model, symmetrically placed in a tetrahedral-like fashion. Equipotential surfaces using different coordinates are given by Michl and co-workers for the H₄ system.⁹ In order to obtain Figure 3 from a calculated potential energy surface we noted earlier that only one quadrant need be computed, since the remaining three are obtained by a permutation symmetry. Similarly, in the three-dimensional global plot only two octants need be computed, one containing a diradical and the other not.

Starting, instead, from any of the diradicals, there are seen in Figure 3 two paths for reaction, one leading to fragmentation to form two ethylenes and the other leading to cyclization to form cyclobutane. Doubleday⁵ recently considered the fragmentation and cyclization of the diradical, noting that the rates

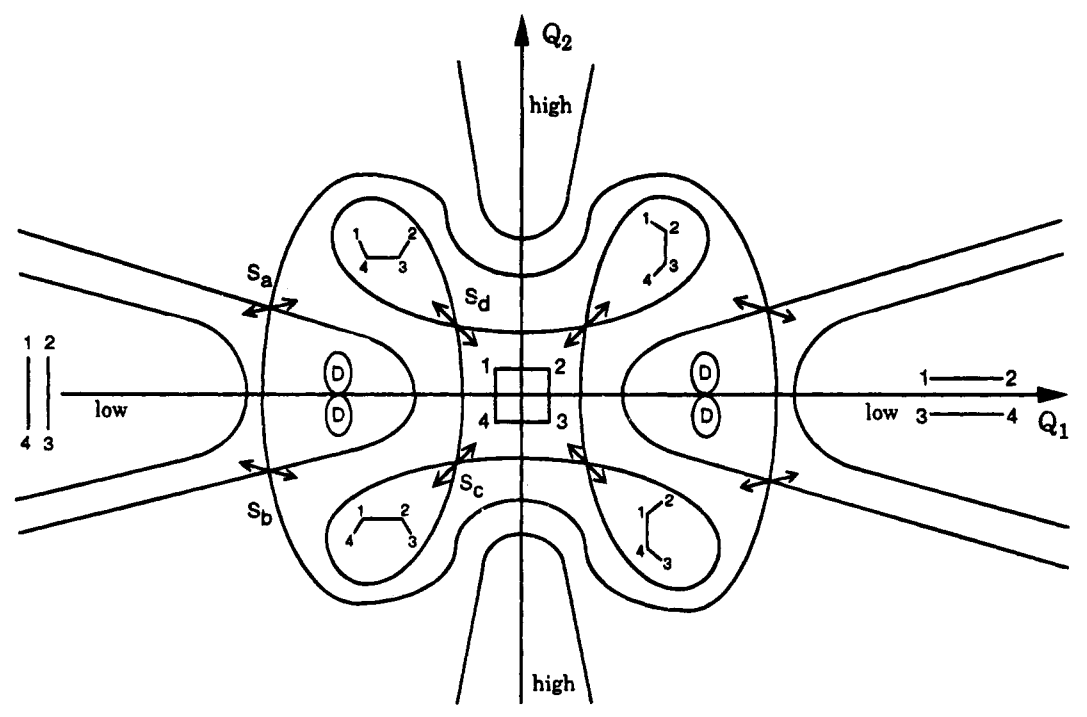


Figure 4. Global contour plot for reactions 1 and 2, when the attachment of the ethylene pairs is gauche.

were independent of the precursor. A second topic, the principal focus of Doubleday's work, is a discussion of the ratios of stereoisomers formed. It involves an analysis of the internal coordinates of the CH₂'s (e.g., ref 5) and so would not be explicitly exhibited in the present global plot. A different plot, focusing on a particular region of Figure 3 and on the CH₂ twisting coordinates, will be considered elsewhere.

Gauche Attachment of the Ethylene Pairs. We comment briefly here on the gauche attachment of the ethylene pairs and the relevant global plot, Figure 4. The concerted face-to-face $[2_s + 2_s]$ addition is Woodward–Hoffmann forbidden, ^{8.9} and involves a conical intersection.³ A more favorable approach is $[2_s + 2_a]$, which has a first-order saddle point⁴ (with a high barrier). In this transition state the angle of torsion of the two ethylenes is calculated ⁴ to be about 40°. The saddle point is depicted in Figure 4, perhaps with domes on each side.

Examination of the relevant structures reveals that new coordinates are needed for the global plot: In the gauche approach atoms 4 and 3 and/or 1 and 2 in Figure 2a become attached. There is now no longer any large internal rotation involved in forming the cyclobutane, and so the atom numbering in the cyclobutane and in the second pair of ethylenes is that given in Figure 4. Also given there are the various gauche attachments to form the diradicals. The appropriate coordinates Q_i for the structures in Figure 4 are now symmetric or antisymmetric with respect to the permutations (24) and (13), instead of (12) and (34). The new coordinates Q_i can therefore be obtained by an argument identical to that given earlier for q_i 's. The result can be written for brevity in a matrix form

$$\mathbf{Q} = \mathbf{A}\mathbf{R} \tag{9}$$

where **Q** and **R** are column vectors with components Q_1 , ..., Q_6 , and r_{34} , r_{12} , r_{23} , r_{14} , r_{13} , r_{24} , respectively. **A**, given in

Appendix A, is an orthogonal matrix and consists of the two block matrices A_1 and A_2 in eq A2.

When there is a face-to-face $[2_s + 2_s]$ approach of the pair of ethylenes in the left side of Figure 4, we have $r_{12} = r_{34}$ and $Q_2 = Q_3 = Q_5 = 0$. A $[2_s + 2_a]$ approach also satisfies these conditions. However, for any given value of Q_1 these two structures occur at two different points in the (Q_4, Q_6) subspace. They differ in their local topology, 3,4 since the $[2_s + 2_a]$ structure occurs at a saddle point and the $[2_s + 2_s]$ occurs at a conical intersection. The condition for face-to-face $[2_s + 2_s]$ approach is $Q_4^2 = Q_6^2$ and, for the $[2_s + 2_a]$ configuration, $Q_4^2 > Q_6^2$. The conical intersection entails a 2-fold barrier to reaction: The cone is high. Its existence also reflects the Woodward-Hoffmann restrictions (nonadiabaticity)^{4,8} and leads to a diversion of the path, so as to go around the cone. In the minimization, the $[2_s + 2_a]$ saddle-point approach is the preferred one and is the one depicted in Figure 4.

Exhibition of the Separatrices. We consider next when and how the separatrices may appear or disappear in a global plot. Only one quadrant of Figure 3 need be considered, e.g., the upper left, as discussed earlier. Analogous remarks apply to the other quadrants and to Figure 4.

We examine first the trans-gauche diradical saddle point, since as discussed earlier only the coordinate r_{13} appears to change significantly in the upper left quadrant on crossing the saddle point along the reaction path (the path for which the saddle point has a negative curvature). All four variables q_1-q_4 contain r_{13} , and whether or not a separatrix appears in the minimized plot depends in the local force constants $\frac{\partial^2 V}{\partial q_i \partial q_j}$ at the saddle point and on the content there of the reaction coordinate (largely r_{13} in the upper left quadrant) in the (q_1, q_2) pair. This appearance or nonappearance of a saddle point in a minimized plot, the global plot, is discussed in Appendix B.

In the case of the cyclization of the gauche diradical, a passage through a saddle point in the upper left quadrant of Figure 3 presumably involves mainly a decrease in the r_{13} coordinate, with a small increase in r_{14} and r_{23} and a small decrease in r_{24} . In the case of the fragmentation of the trans diradical (saddle point S_d in Figure 3) the r_{24} in Figure 2c increases, with a smaller

⁽⁸⁾ Kash, R. W.; Waschensky, G. C. G.; Moras, R. E.; Butler, L. J.; Franci, M. M. J. Chem. Phys. 1994, 100, 3463. Waschensky, G. C. G.; Kash, R. W.; Myers, T. L.; Kitchen, D. C.; Butler, L. J. J. Chem. Soc., Faraday Trans. 1994, 90, 1581.

⁽⁹⁾ Gerhartz, W.; Podhusta, R. D.; Michl, J. J. Am. Chem. Soc. 1976, 98, 6427. Cf.: Michl, J.; Bonacic-Koutecky, V. Electronic Aspects of Organic Photochemistry; Wiley: New York, 1990; pp 244-245.

decrease in r_{14} and r_{23} ($r_{14} = r_{23}$). Once again, the appearance of a separatrix in each case depends on the properties mentioned above.

G(T,q) or S(E,q) Curves

We consider next the plots of thermodynamic properties along a reaction coordinate q, in particular the plot of a free energy G(T,q) in a canonical system, i.e., a system at temperature T, or the entropy S(E,q) in an isolated molecule, i.e., a microcanonical system of energy E and total angular momentum J. We first note that each diradical has a significant entropy compared with the cyclo C₄ compound, since the former has a number of internal rotations. The various coordinates not specified in Figure 3, i.e., the 4 remaining coordinates of the four carbons and the 24 other coordinates of the four methylenes, contribute to the entropy. Thus, in addition to any potential energy well of the diradical in Figure 3, there is an entropic contribution to a "free energy" well. To calculate G(T,q) or S(E,q) appropriate statistical ensembles are used, as noted later.

When the transition state is "tight", i.e., has only smallamplitude vibrations, and when there is a fairly peaked maximum of the potential energy V along the reaction path, the choice of the reaction coordinate q and its value q^{\dagger} in the transition state and the calculation of the properties of the transition state, $G(T,q^{\ddagger})$ or $S(E,q^{\ddagger})$, are standard. Only when there is some flexibility in the motions transverse to the reaction coordinate, e.g., when there are large-amplitude internal rotations and when V is not strongly peaked at some q, does one need to use a variational type of transition state theory, as well as to choose with care the nature of q. Such flexible systems were the subject of a series of recent papers on RRKM theory and its variational form (cf. refs 10 and 11 and references cited therein).

We consider this "nontight" or "flexible" transition state theory 10,11 next. In plots of G(T,q) or S(E,q) versus a reaction coordinate q, one task is to define q. Its nature will differ for the different paths in reactions 1 and 2. When a particular reaction coordinate q is introduced, e.g., from the left-hand valley to the upper left diradical region, i.e., for the first step in reaction 2, it defines a family of hypersurfaces, each differing in its value of q. Various choices of q, and indeed optimum choices of q among a class of reaction coordinates, for obtaining a rate constant have been discussed by Klippenstein, 12 and we refer the reader to his work.

Given some choice of the nature of q, not yet the best choice, one can calculate by statistical mechanics in the canonical case the free energy G(T,q) for each member of the family of hypersurfaces, i.e., for each value of q. For the canonical case we have

$$k(T) = \min_{q} \frac{kT}{h} e^{-[G(T,q) - G^{\dagger}(T)]/kT}$$
(10)

where G(T,q) is the free energy as a function of q at the given temperature T and $G^{r}(T)$ is the free energy of the reactants. This expression for variational transition state theory has a long history (cited in ref 10), and its fullest exposition and application is given in articles by Truhlar and co-workers (e.g., ref 13).

The best choice of the form q will make k(T) as small as possible when the form¹² of q and the value^{10–12} of q itself are both varied. In terms of Wigner's concept¹⁴ of a transition state, the optimum form and value of q is the one for which the system

makes the fewest recrossings of the transition state. His ideas represented a dynamical advance over the more user friendly ones of Eyring¹⁵ and of Evans and Polanyi.¹⁶

In the microcanonical case one can calculate N(E,J,q), the number of quantum states, as a function of q. This N(E,J,q) is related to the corresponding entropy S(E,J,q) by the Boltzmann expression,

$$S(E,J,q) = k \ln N(E,J,q) \tag{11}$$

The rate constant k(E,J) is given by the variational RRKM value (cf. refs 10, 11, 17 and references cited therein).

$$k(E,J) = \min_{q} N(E,J,q)/h\varrho(E,J)$$
 (12)

where ϱ denotes the density of states of the parent molecule. The actual k(E,J) is obtained, as indicated in eq. 11, by choosing q so as to minimize N(E,J,q). This choice for k(E,J) can be termed variational RRKM theory, having been first introduced in this context¹⁷ (cf. also footnote 10 of ref 10). It may be recalled that RRKM theory is the microcanonical form of transition state theory: The transition state theory of Eyring¹⁵ and of Evans and Polanyi¹⁶ was designed for a reaction at constant temperature. In formulating RRKM theory, 18 the idea of a transition state was combined with the statistical RRK (Rice, Ramsperger, Kassel) concepts of the 1920s and used to describe the reactive behavior of molecules of energy E.

The G(T,q) or S(E,J,q) appearing in eqs 10-12 are defined using a hypersurface, i.e., using an (n-1)-dimensional subspace in an n-dimensional space. Each hypersurface of a family is characterized by a value of q. One of these, at $q = q^{\dagger}$, constitutes the transition state of the reaction and, in the case of the tight transition state, passes through the saddle-point region separating the reactants from the products. Thus, when the transition state is "tight", the choice of the nature of q and of its value of q^{\dagger} in the transition state is standard (the minimization would yield a q^{\dagger} in which the saddle point is on the hypersurface $q = q^{\ddagger}$). Equations 9 and 11 can be simplified, thereby, by omitting the "min" and replacing q by this q^{\ddagger} .

The method of choosing a suitable family of hypersurfaces becomes challenging when there is no marked potential energy maximum (and so no marked saddlepoint) along the reaction path. A method of taking into account the role of many lowfrequency coordinates and choosing the transition state was the focus of recent studies on the variational form of RRKM theory. 10-12,17,19 As noted earlier, an insightful choice of the optimum in a class of q's is treated in the recent work of Klippenstein.¹²

There are seen in Figure 3 several reaction coordinates q, one for each reaction. The q in reaction 2 leads from the upper left diradical region through the neck to the central potential energy minimum. The reaction coordinate for the concerted reaction, reaction 1, leads instead directly from the left valley to the central well, but in Figure 4 it is typically diverted to either side of the conical intersection D, to avoid the highest energy regions and to enhance the "adiabaticity" (the act of staying on a single potential energy surface, here the lowest).

(15) Eyring, H. J. Chem. Phys. 1935, 3, 107.

⁽¹⁰⁾ Wardlaw, D. M.; Marcus, R. A. Adv. Chem. Phys. 1987, 70 (Part 2), 231.

⁽¹¹⁾ Klippenstein, S. J.; Marcus, R. A. J. Phys. Chem. 1990, 93, 2148.

⁽¹²⁾ Klippenstein, S. J. Chem. Phys. Lett. 1994, 214, 418.

⁽¹³⁾ Truhlar, D. G.; Isacson, A. D.; Garrett, B. C. In Theory of Chemical Reaction Dynamics; Baer, M., Ed.; CRC Press: Boca Raton, FL, 1985;

⁽¹⁴⁾ Wigner, E. Trans. Faraday Soc. 1938, 34, 29.

⁽¹⁶⁾ Evans, M. G.; Polanyi, M. Trans. Faraday Soc. 1935, 31, 875.

⁽¹⁷⁾ Marcus, R. A. J. Chem. Phys. 1966, 45, 2630.

⁽¹⁸⁾ Marcus, R. A.; Rice, O. K. J. Phys. Colloid Chem. 1951, 55, 894. Marcus, R. A. J. Chem. Phys. 1952, 20, 359.

⁽¹⁹⁾ Klippenstein, S. J.; Kress, J. D. J. Chem. Phys. 1992, 96, 8164. Klippenstein, S. J. Ibid. 1992, 96, 367. Wardlaw, D. M.; Marcus, R. A. Chem. Phys. Lett. 1984, 110, 230.

It is evident from this description that there are three distinctly different reaction coordinates in reactions 1 and 2. Thus, one should not draw, as one might be tempted to do, the entropy S(E,J,q) or free energy G(T,q) versus reaction coordinate curve for reaction 1 on the same plot as the corresponding curve for either of the two steps in reaction 2. In any comparison of plots of entropy or free energy curves versus a coordinate q for two systems, as in the free energy curves for weak overlap electron transfers, the ensemble of configurations selected should be identical for the two curves, if the comparison is to be meaningful. This latter consideration was especially important in constructing free energy curves vs reaction coordinate for electron transfer reactions.²⁰

On a somewhat different topic, we also note that any isomerization of one diradical into another, e.g., from the upper left region in Figure 3 to the upper right, is impeded in that figure both by there being a barrier en route and by the trajectory proceeding on the side of a hill. It would tend, in the process, to become diverted into the C_4 minimum.

Second- and Higher-Order Saddle Points

Among the other topographical features of a surface are the second- and higher-order saddle points, i.e., saddle points which have two or more negative eigenvalues for the local force constant matrix (the Hessian), whereas an ordinary saddle point has only one. As noted in ref 4 a second-order saddle point found there had no particular chemical significance, but we comment briefly on it and on domes.

A second-order saddle point was found⁴ for the rectangular transition-like structure ($\alpha_1 = \alpha_2 = \pi/2$) and for the trapezoidal structure ($\alpha_1 = \alpha_2 \neq \pi/2$) in a topographical map of V in a restricted subspace. The V was a maximum at $\varphi = 0$, i.e., $\partial V / \partial \varphi = 0$ and a negative value for $\partial^2 V / \partial \varphi^2$. It yielded the second negative eigenvalue for the force constant matrix in this subspace. Subsequent variation of φ yielded a φ for which $\partial V / \partial \varphi = 0$ and a positive value for $\partial^2 V / \partial \varphi^2$. The point so reached was now a local minimum, as a function of φ , and was the (first-order) saddle point for the following reaction: ethylene pair \rightarrow diradical. In a topographical map in ref 4 (Figure 7 there), the second-order saddle point appears topographically as a first-order saddle point, but only because φ was held fixed in the map.

If a dome, rather than a conical intersection, appears after a minimization then it is a second-order saddle point in the minimized plot and serves to divert a reaction path, as in Figures 3 and 4.

Summary and Concluding Remarks

The global plot is intended to present an overall picture of the various processes, their relationship with each other, and the overall topography of the surfaces, such as the minima, the saddle points, and conical intersections. As such it is complementary to usual contour or topographical plots, which are 2-dimensional cuts of the potential energy surface in the many-dimensional coordinate space and which focus on local regions of that coordinate space. A different type of plot is one in which a profile of the potential energy surface for the cyclization of the diradical and the profile for the fragmentation are plotted versus the same reaction coordinate. The plots in Figures 3 and 4 make it very clear that the reaction coordinates for the processes are very different, and hence that the above 1-D plot is incorrect. A potential shortcoming of the global plot is a possible distortion of a surface feature such as a saddle point

as a result of the minimization process. It will be interesting to see how the global plot appears in an actual calculation using an *ab initio* surface.

In ref 1 a global plot was used to explore why one of the transition states for an H₃O system, not previously located in an ab initio calculation of the potential energy surface, was not found. It is perhaps too much to expect in a reaction so well studied as the concerted vs stepwise cycloaddition of two ethylenes that the new type of plot will provide new insights. One feature which emerges from Figures 3 and 4 concerns the comparison between a concerted and a stepwise process: The comparison will differ, depending on whether a trans or a gauche attachment of the ethylenes is considered in the stepwise reaction: In the trans attachment, the appropriate concerted reaction according to Figure 3 is a $[2_s + 2_a]$ reaction which occurs along the q_1 axis in Figure 3 and thereby involves an unusually large internal rotation, the twisting of one ethylene with respect to the other to reach the cyclobutane configuration. The formation of the diradical via a gauche attachment, on the other hand, should be compared with a $[2_s + 2_s]$ cycloaddition and with a different $[2_s + 2_a]$ cycloaddition, one having a relatively small twist of the two ethylenes (Figure 4). Figure 3 suggests that the dome diverts a concerted ethylene—ethylene attachment into becoming an attachment which forms instead a diradical, while in Figure 4 the same effect occurs unless the alignment is close enough that the system proceeds so close to the q_1 axis that it passes through the saddle point indicated there on that axis. (However, as a precautionary note, it should be stressed that, at present, Figures 3 and 4 are drawn in the absence of a detailed calculation of the minimized surface.)

From the usual contour plots for collinear $A + BC \rightarrow AB + C$ reactions there have been new insights, as in the dynamical basis of vibrational adiabaticity using reaction coordinates²¹ based on the topography of the potential energy surface, and dynamical concepts such as those used in early and late downhill reactions.²² For other systems, too, it may be anticipated that the detailed dynamics will again depend on details such as curvatures,²¹ change of vibrational frequencies²¹ and torsions along an actual reaction path in the original N-dimensional space, and factors related to angular momentum restrictions; but an initial overall picture may be provided by the global plot.

Acknowledgment. It is a pleasure to acknowledge the support of this research by the National Science Foundation and the very helpful comments of John Baldwin.

Appendix A. Transformation of Coordinates and Inverse Transformation

The coordinate transformation given by eqs 3-8 can be written in matrix form as

$$\mathbf{q} \equiv \begin{bmatrix} q_1 \\ q_2 \\ q_3 \\ q_4 \\ q_5 \\ q_6 \end{bmatrix} = \begin{bmatrix} \mathbf{A}_1 & \mathbf{O} \\ \mathbf{O} & \mathbf{A}_2 \end{bmatrix} \begin{bmatrix} r_{23} \\ r_{13} \\ r_{24} \\ r_{14} \\ r_{12} \\ r_{34} \end{bmatrix} \equiv \mathbf{Ar} \tag{A1}$$

where A_1 is a symmetric orthogonal matrix and A_2 is a rotation

⁽²¹⁾ Marcus, R. A. J. Chem. Phys. 1966, 45, 4500. Marcus, R. A. Ibid. 1965, 43, 1598.

⁽²²⁾ E.g.: Anlauf, K. G.; Kuntz, P. J.; Maylotte, D. H.; Pacey, P. D.; Polanyi, J. C. *Discuss. Faraday Soc.* 1967, 44, 183 and references cited therein. Laidler, K. J. *Theories of Chemical Reaction Rates*; McGraw-Hill: New York, NY, 1969; pp 178-182.

matrix

It is readily verified that

$$\mathbf{A}_1^{-1} = \mathbf{A}_1, \quad \mathbf{A}_2^{-1} = \mathbf{A}_2^{\mathrm{T}} \tag{A3}$$

where T denotes the transpose. Thereby, one finds that

$$r_{23} = \frac{1}{2}(q_1 - q_2 - q_3 + q_4) \tag{A4}$$

$$r_{13} = \frac{1}{2}(-q_1 + q_2 - q_3 + q_4) \tag{A5}$$

$$r_{24} = \frac{1}{2}(-q_1 - q_2 + q_3 + q_4) \tag{A6}$$

$$r_{14} = {}^{1}/_{2}(q_{1} + q_{2} + q_{3} + q_{3}) \tag{A7}$$

$$r_{12} = \frac{1}{\sqrt{2}}(q_5 + q_6) \tag{A8}$$

$$r_{34} = \frac{1}{\sqrt{2}}(q_5 - q_6) \tag{A9}$$

We note in passing that the transformation is "distance conserving":

$$\mathbf{q}^{\mathsf{T}} \cdot \mathbf{q} = \mathbf{r}^{\mathsf{T}} \mathbf{A}^{\mathsf{T}} \cdot \mathbf{A} \mathbf{r} = \mathbf{r}^{\mathsf{T}} \cdot \mathbf{r} \tag{A10}$$

Appendix B. Saddle-Point Regions and Their Survival

We consider the behavior of a potential energy surface and the minimized surface in the vicinity of a first-order saddle point S of the original surface.

Regardless of the coordinates used, a diagonalization of the force constant matrix (the Hessian) yields, in the vicinity of the saddle point,

$$V = V_0 - \frac{1}{2}k_1x_1^2 + \frac{1}{2}\sum_{i=1}^{n}k_ix_i^2$$
 (B1)

Here, V_0 is the value of V at the saddle point $x_1 = ... = x_n = 0$. The coefficients $-k_1, k_2, ..., k_n$ are the curvatures of the surface at S, the k_i 's being all positive. In the case of n = 2, the contour lines in (x_1,x_2) space, i.e., the lines of V = constant, are the hyperbolae, $\frac{1}{2}k_2x_2^2 - \frac{1}{2}k_1x_1^2 = V - V_0$. The contour lines passing through S have $V = V_0$, and hence consist of two such lines, $\sqrt{k_1x_1} \pm \sqrt{k_2x_2} = 0$, as in Figure 3 or 4, for example. They form the two arms of the separatrix. When V is minimized with respect to the coordinates $x_3, ..., x_n$, this n = 2 case results.

On the other hand, if neither of the coordinates (x_1,x_2) used as axes in the 2-D global contour plot contains the reaction coordinate, which will be denoted now by x_3 , we would have

$$V = V_0 + \frac{1}{2} \sum_{i \neq 3} k_i x_i^2 + V(x_3)$$
 (B2)

where $V(x_3)$ is a double well potential energy function with a leading term $-\frac{1}{2}k_3x_3^2$ at the saddle point. The $V(x_3)$ has minima at x_3^+ and x_3^- , according to $x_3 > 0$ or $x_3 < 0$. One then sees the minimizing V with respect to the x_i for i > 2 leads to

 $x_i = 0$ for i > 3 and the lower of the two minima:

$$V(\text{minimized}) = V_0 + \frac{1}{2}(k_2 x_2^2 + k_1 x_1^2) + V(x_3^{\pm})$$
 (B3)

where $V(x_3^{\pm})$ is the smaller of $V(x_3^{+})$, which is the minimum when $x_3 > 0$, and $V(x_3^{-})$, which is the minimum when $x_3 < 0$. Thus, in this case, the separatrix has not survived the minimization.

We consider next the more general case which is intermediate between the above two extremes. We let the local reaction coordinate (the coordinate associated with the negative curvature) contribute both to the (q_1,q_2) pair and to the variables involved in the minimization. For notational brevity all coordinates q_i (and x_i) are now defined relative to their values at the saddle point. For simplicity of presentation we suppose that both the reaction coordinate x_1 and another coordinate x_3 contribute to q_1 and q_3 and consider the more general case later:

$$2V = 2V_0 - x_1^2 + \omega_2^2 q_2^2 + \omega_3^2 x_3^2$$
 (B4)

plus a term which contains the other coordinates.

We relate x_1 and x_3 to q_1 and q_3 by an orthogonal transformation:

$$x_1 = (q_1 + aq_3)/(1 + a^2)^{1/2}$$
 (B5)

$$x_3 = (-aq_1 + q_3)(1 + a^2)^{1/2}$$
 (B6)

Minimizing V with respect to q_3 yields

$$x_3 = ax_1/\omega_3^2 \tag{B7}$$

so that now the V for the minimized plot is

$$2V(\text{minimized}) = -(1 - a^2/\omega_3^2)x_1^2 + \omega_2^2q_2^2$$
 (B8)

where q_i (and x_i) can be expressed in terms of q_1 using eqs B5-B7. Thus, the saddle point survives the minimization only if the coefficient of x_1^2 in parentheses is positive, i.e., provided $a^2 < \omega_3^2$. That is, there is a survival only if the local reaction coordinate x_1 does not contribute too greatly to the minimized variable q_3 , the fraction allowed being weighted by $1/\omega_3^2$, the ratio of the negative force constant of the reaction coordinate x_1 motion to the force constant for the x_3 coordinate.

The result is immediately extended to many variables: The potential energy V can be written as

$$V = V_0 + \frac{1}{2} \mathbf{q}^{\mathsf{T}} \mathbf{K} \mathbf{q} \tag{B9}$$

in the vicinity of the saddle point. The vectors and matrices can be written as

$$\mathbf{q} = \begin{bmatrix} \mathbf{q}_{a} \\ \mathbf{q}_{b} \end{bmatrix} \quad \mathbf{K} = \begin{bmatrix} \mathbf{K}_{aa} & \mathbf{K}_{ab} \\ \mathbf{K}_{ba} & \mathbf{K}_{bb} \end{bmatrix}$$
(B10)

where \mathbf{q}_a is a vector with components q_1 and q_2 , \mathbf{q}_b has components q_3 , ..., q_n , \mathbf{K}_{aa} is a symmetric 2×2 matrix, and \mathbf{K}_{bb} is a symmetric $N-2 \times N-2$ matrix.

On minimizing V and solving for \mathbf{q}_b in terms of \mathbf{q}_a one obtains $\mathbf{q}_b = -\mathbf{K}_{bb}^{-1} \mathbf{K}_{ba} \mathbf{q}_a$ and from it

$$V = V_0 + {}^{1}/_{2} \mathbf{q}_{a}^{T} [\mathbf{K}_{aa} - \mathbf{K}_{ab} \mathbf{K}_{bb}^{-1} \mathbf{K}_{ba}] \mathbf{q}_{a}$$
 (B11)

The saddle point survives the minimization if the matrix in brackets has a negative eigenvalue.

JA9434386